Isolation and structural characterization of cellulose from *sericostoma pauciflorum*

[1]Jitubhai Morabiya[a*], [2]Hardik Bhatt[b], [3]Sanjay Bamaniya[a]

[a]Department of Chemistry, Bhakta Kavi Narsinh Mehta University, Junagadh, Gujarat, India.

[b]SET Science College and PG Centre, Department of Chemistry, Junagadh, Gujarat, India.

*Corresponding Author's Email: jitubhamorabiya@gmal.com

Abstract

Cellulose is one of the most prevalent and cost-free natural polymers on Earth and plays a crucial structural role in plant cell walls. Isolating and chemically characterizing cellulose can benefit various industries by enabling them to utilize its potential fully. This study reports cellulose extraction from *Sericostoma Pauciflorum* through a process involving bleaching followed by alkali and acidic treatments. The crude cellulose obtained was further fractionated into alpha (α) and beta (β) cellulose fractions. Structural analyses were performed using Fourier Transform Infrared Spectroscopy (FTIR) and X-ray Diffraction (XRD). The morphology and thermal stability of the crude, α, and β cellulose were examined using Scanning Electron Microscopy (SEM) and Thermogravimetric Analysis (TGA), respectively. The cellulose yield from *Sericostoma Pauciflorum* was found to be 82%, with the α and β cellulose fractions comprising 83.6% and 8.2%, respectively. This indicates that α-cellulose predominates in *Sericostoma Pauciflorum*. Morphological studies, FTIR, and SEM analyses confirmed the successful extraction of cellulose and showed that the alkali and acidic treatments effectively removed most of the Crude cellulose and lignin. XRD analysis further confirmed that all samples exhibited a cellulose I polymorph structure, with no evidence of cellulose II. The crystallinity index and crystallite size of β-cellulose (79.10% and 51.67 nm, respectively) were higher than those of α-cellulose (63.05% and 18.54 nm). Additionally, the crystallinity of fractionated β-cellulose (79.10%) was greater than that of crude cellulose (71.35%), suggesting that β-cellulose exists in a more ordered form. Thermogravimetric analysis demonstrated that β-cellulose had significantly higher thermal stability than α-cellulose, with thermal decomposition rates in the temperature range of 200-600°C of 70.39% for α-cellulose and 2.02% for β-cellulose. Overall, the results were consistent with existing literature, providing valuable insights that could inform future research and applications in various fields.

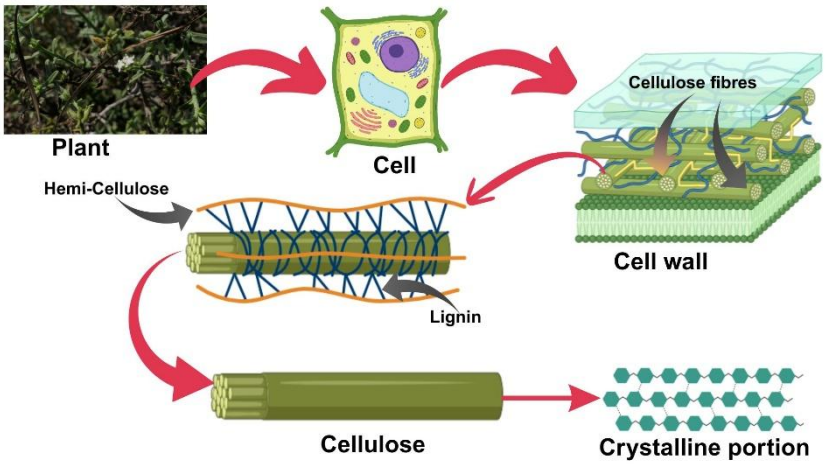

Keywords: *Sericostoma pauciflorum*, α-cellulose, β-cellulose, Fractionation, Acid-Alkali treatment

1. Introduction

Cellulose is a naturally occurring, Renewable feedstock [1] biopolymer found in the cell walls of all plants and trees.[2] It is cost-free, Eco-friendly [3] and biodegradable [4], useful materials for paper mills, biofuel, and are now also used as supportive materials in light-harvesting devices [5]. Due to all the above properties, cellulose would be more important or might be a replacement for toxic, hazardous polymers. Structurally, cellulose unbranched, linear biopolymer [6] formed from β-D-Glucose unit which are joined by β-1,4-Glycosidic link [7] and form a homopolymer-like structure. Isolation of cellulose has already been done in many attempts, such as Brewer spent grain [8] Corn stover [9] Raw kenaf [10] Poplar sawdust [11] Jute [12], Sugarcane bagasse [13] other sources of cellulose include agricultural waste, residue like Maize, Rice, Wheat straw, etc. [14]

Since cellulose nanofibers significantly enhance the mechanical properties of polymers, there has been a significant spike in interest in using them as strengthening agents. The conversion of cellulose nanocrystals is frequently accomplished by acid hydrolysis [15] such as that involving sulfuric, phosphoric, or hydrochloric acid [16]. Because of their unique chiral nematic geometry, these nanocrystals exhibit remarkable optical properties and react to a range of environmental stimuli [17]. Cellulosic materials can be combined with functional polymers, small molecules, and other nanomaterials to introduce a variety of new functionalities and improve and stabilize responsive optical signals [18] Integrating cellulosic materials with functional polymers, small molecules, and various nanomaterials can enhance and stabilize responsive optical signals while introducing a range of new functionalities. Techniques for surface modification can resolve compatibility issues between nanocellulose and polymeric materials, thereby improving uniformity and interfacial interactions. Cellulose-based nanomaterials find applications in chemical sensors, photonic papers, and drug delivery systems, leveraging their biocompatibility and favourable physical and chemical properties [19]. The cellulose industry relies heavily on lignocellulosic biomass sources such as wood, cotton, flax, hemp, and jute for cellulose production [20]. A significant challenge in extracting cellulose from lignocellulosic biomass is the removal of lignin [21]. The harsh chemical treatment of biomass can lead to partial degradation of cellulose and produce effluents with significant environmental concerns. Consequently, easily accessible and rapidly growing biomass like seaweeds is gaining global attention as an additional cellulose source [22] which possesses remarkable properties similar to plant cellulose. And many other evidence is also available, such as wastewater treatment [23], light-harvesting devices [24], Renewable energy [25], biosorbents for hazardous metals, Dyes, pollutants, in short, organic and inorganic materials [26], Tissue engineering, and Biosensors [27,28]

Numerous researchers have undertaken the task of isolating cellulose from various methods and sources to examine their characteristic properties. In this context, we have initially endeavoured to isolate cellulose and conduct a fractionation process on *Sericostoma pauciflorum*. Consequently, this study was effectively executed to fractionate native cellulose utilizing a cost-efficient and dependable methodology, while also

analysing the chemical characterization of the fractionated cellulose to explore its potential applications across various domains proficiently.

2. MATERIALS AND METHODS

2.1 Raw materials

The species *Sericostoma Pauciflorum* is particularly abundant in Gujarat's Junagadh district, India, due to the easy availability of this plant for my work. Known locally as "Karvas," the leaves of *Sericostoma Pauciflorum* are valued for their medicinal properties. Plant samples were collected from the forested areas of Junagadh District between May 2022 and July 2022. Methanol was used to achieve depigmentation rather than Sodium acetate (CH_3COONa), Sodium chlorite ($NaClO_2$), Sodium hypochlorite (NaOCl), Sodium Hydroxide (NaOH), and Sulphuric Acid were also used for the purification process. Which is purchased from Sisco Research Laboratory, Mumbai, India.

2.2 *Isolation of cellulose*

Mihranyan et al.'s approach [29] was implemented in the technique of cellulose extraction from *Sericostoma Pauciflorum*. Before being crushed into a finer form, *Sericostoma Pauciflorum* specimens were cleaned first with normal drinking water in order to obtain rid of any contaminants or sediment. They were subsequently allowed to dry in the shade. 100 grams of this dehydrated plant-based powder were taken out repeatedly over a period of 8 days (2 days each round) at ambient temperature in an attempt to defat it with 500 millilitres of methanol. The dehydrated powder of plants was immersed for three hours at 60°C in one litre of buffered acetate, which contained 36 grams of sodium chlorite ($NaClO_2$) as part of the bleach procedure. The neutral pH of about 7 was attained by washing the bleached materials with tap water. Following that, 600 mL of a 0.5 M NaOH solution was then added to the bulk, and it was allowed to sit nightly at 60°C. The material that was previously alkali-treated was then passed through filters and allowed to air out at the ambient temperature, and finally rinsed with water until the pH became neutral. After heating the air-dried matter with 200 millilitres of 5% v/v HCl, the solution was heated to a boil and left to settle at the ambient temperature over the whole night. The unused acid was then washed away with water, filtered, and dried to remove cellulose. In order to obtain the removal of any remaining unfavourable pigments, the final product was bleached again with sodium hypochlorite. The final yield was determined using the original amount of plant powder.

2.3 Fractionation of cellulose

Siddhanta et al.'s examination [30] was applied to separate α and β-cellulose from crude cellulose. For two hours, the dried cellulose was maintained at 20°C while being mixed after fifteen minutes, in 30 mL of a 17.5% NaOH solution was used. Following that, the produced pulp went through a centrifuge for 15 minutes at a rate of 8000 rpm. Whereas a solution having β-cellulose has been separated by decanting. the α-cellulose remains insoluble, remains behind 3N H_2SO_4 (30 ml) was employed for precipitating the β-cellulose from the solution. The mix was brought up to 80°C for 10 minutes for the purpose of ensuring total precipitation. A centrifuge was applied to separate the precipitated β-cellulose, and it was filtered with water. and dried in a freeze-drier. Furthermore, the α-cellulose was extracted, cleansed to a pH of 7, and finally dehydrated in a freeze dryer. The extracted residue from plants was used to determine yield. Additionally, see the flow chart in **fig.1**

Fig. 1 Flow chart of Separation of Crude cellulose, α-cellulose, and β-cellulose.

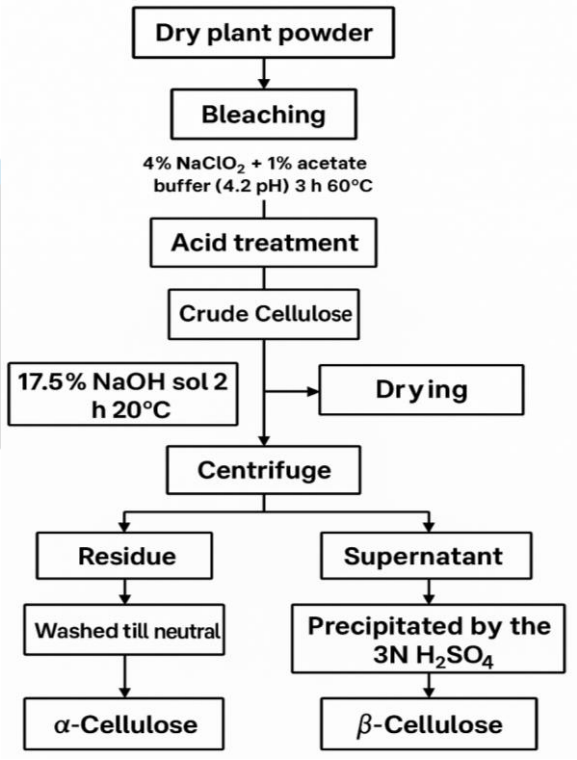

2.4 Characterization of α, β, and Crude Cellulose

Characterization of the isolated cellulose was performed using various analytical techniques to assess its purity, structural properties, and potential applications.

A Japanese HITACHI-SU8010 scanning electron microscope (SEM) was used to investigate the microstructure of cellulose (Crude cellulose, α-cellulose, and β-cellulose). The samples were seen at an acceleration voltage of 70 kV and a resolution of ×202.

The Fourier transform infrared (FTIR) spectra of Crude cellulose, α-cellulose, and β-cellulose have been obtained using Shimadzu-IRA affinity-1 to investigate any possible chemical interactions found in cellulose samples. 10.0 mg of each finely chopped cellulose sample was incorporated with 500 mg of KBr matrix, and the entire mixture was compressed to form pellets.

Powder X-ray diffraction examinations employing 2θ = 5° to 80° have been performed using an Empyrean, Malvern Panalytical (Netherlands) X-ray powder diffractometer. For figuring out the crystallinity index (C.I.), apply the formula (a) given by Parihar et al. [31]

$$\text{Crystallinity Index}(\%) = [(I_C - I_{NC}/I_C)] * 100 \ldots (1)$$

Where;

I_C = The peak with the highest intensity of the crystalline part

I_{NC} = the peak with the lowest intensity of the amorphous region.

Crystallite size (V) was calculated using Scherrer Eq. (b) reported by Patterson[32].

$$D = K\lambda / \beta \cos\theta \ldots (2)$$

Where,

K = constant (0.9)

λ = X-ray wavelength (0.154 nm),

θ = Bragg's angle

β = the intensity of the (FWHM) corresponding to a high-intensity peak of the diffraction plane 002.

TGA of cellulose samples was performed with NETZSCH-Libra TGA209F1D-1, at a temperature range from 25°C to 800°C at a heat at 10.0 K/min in a Nitrogen atmosphere. The obtained result was used to assess the stability of α- and β-cellulose towards temperature variation.

3. RESULTS AND DISCUSSION

3.1 Isolated cellulose yield

The obtained yield was 82% of Crude cellulose isolated from *Sericostoma pauciflorum,* while further separation yielded 83.6% and 8.2% of α and β-cellulose, respectively. This indicates α-cellulose is more dominant compared to β-cellulose in our chosen plant.

Crude cellulose yield is determined based on the amount of defatted plant residue, according to Parihar et al. [31]

Equation(c) is given below.

$$\text{Crude Cellulose } (\%) = M_{crude}/M_{residue} * 100 \ldots\ldots\ldots (3)$$

Where;

M_{crude} = obtained crude cellulose mass,

$M_{residue}$ = defatted *Sericostoma Pauciflorum* plant residue

While % yield of α and β-cellulose was determined by the amount of Crude cellulose extracted from *Sericostoma Pauciflorum* using Eq. (d) and Eq. (e), respectively.

$$\alpha \text{ Cellulose } (\%) = M_{\alpha}/M_{crude} * 100 \ldots\ldots\ldots\ldots\ldots (4)$$

$$\beta \text{ Cellulose } (\%) = M_{\beta}/M_{crude} * 100 \ldots\ldots\ldots\ldots\ldots (5)$$

Where;

M_{α} = α-cellulose mass

M_{β} = β-cellulose mass

3.2 Morphology assessment by SEM

Fig. 2. Gives information on the surface analogy of different cellulose samples isolated from *Sericostoma Pauciflorum*. The SEM micrographs of Crude and α-cellulose (Fig. 2A and Fig. 2C) indicate the presence of separated fibrils, which suggests the removal of Crude cellulose and lignin deposition on the surface [32]. Furthermore, the micrographs of β-cellulose as represented in Fig. 2B were found to have more ordered structures.

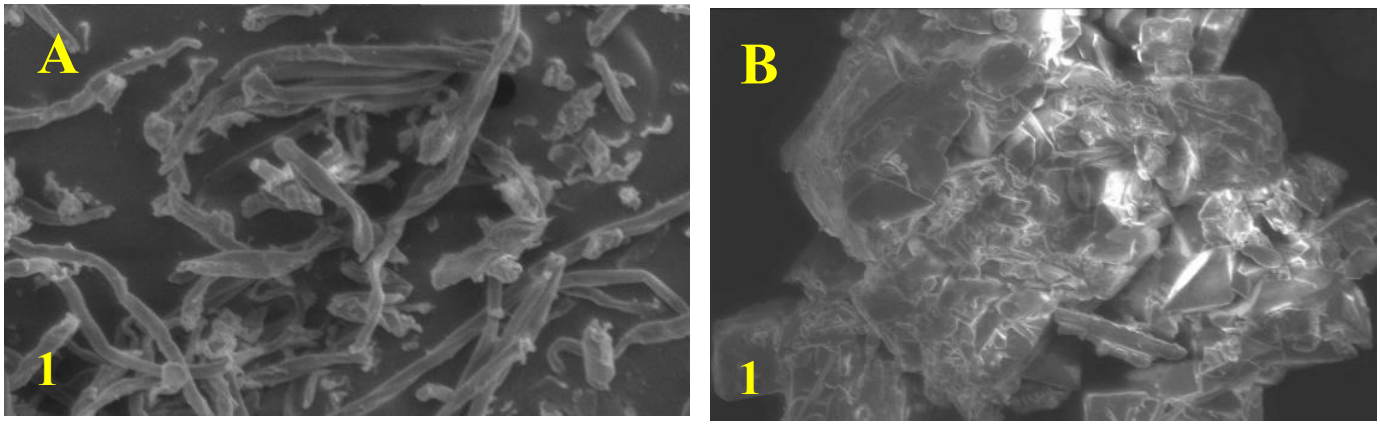

Figure 2. SEM micrograph of (A) α-cellulose, (B) β-cellulose, (C) Crude cellulose

C

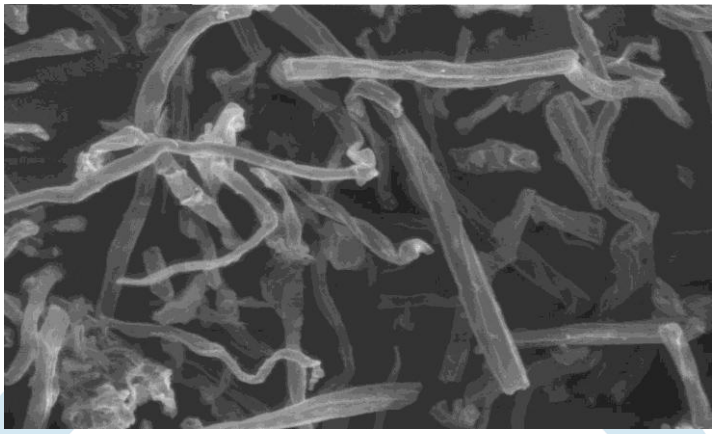

s

3.3 Fourier transform infrared spectral (FTIR) analysis of cellulose

The FTIR spectra of the Crude, α, and β-cellulose obtained from *Sericostoma Pauciflorum* were in good agreement with the reported cellulose and are presented in **Fig. 3**. The dominant broad and intense peak around 3500-3700 cm^{-1} in all infrared spectra of the samples is attributed to the stretching vibration of the OH group, and the peak at 2900-3050 cm^{-1} is associated with the CH stretching vibration of cellulose.[33] The OH bending of the water that is soaked in the cellulose correlates to the absorption peaks showing up in the 1700-1710 cm^{-1} region.[34] CH_2 bending vibration has been associated with the peaks at 1450-1520 cm^{-1}. The C-O-C asymmetric stretching of the cellulose and the internal vibration of the C-O-C pyranose cyclic framework in the cellulose are the causes of the maxima at 1170 and 1000 cm^{-1}, accordingly [35]. The FTIR analysis of the β-cellulose shows a peak 840 cm^{-1}, which is caused by the glycosidic link of β (1→4) cellulose [36]. The lack of lignin or uronic ester linkage with hemicellulose acetyl groups is apparent by the absence of the shoulder peak at 1735 cm^{-1}. Similarly, the lack of the C=C of the aromatic structure of lignin is shown by the absence of the peak at 1540 cm^{-1}[35]. Therefore, the FTIR spectra support the pure state of cellulose and confirm the lack of hemicellulose and lignin.

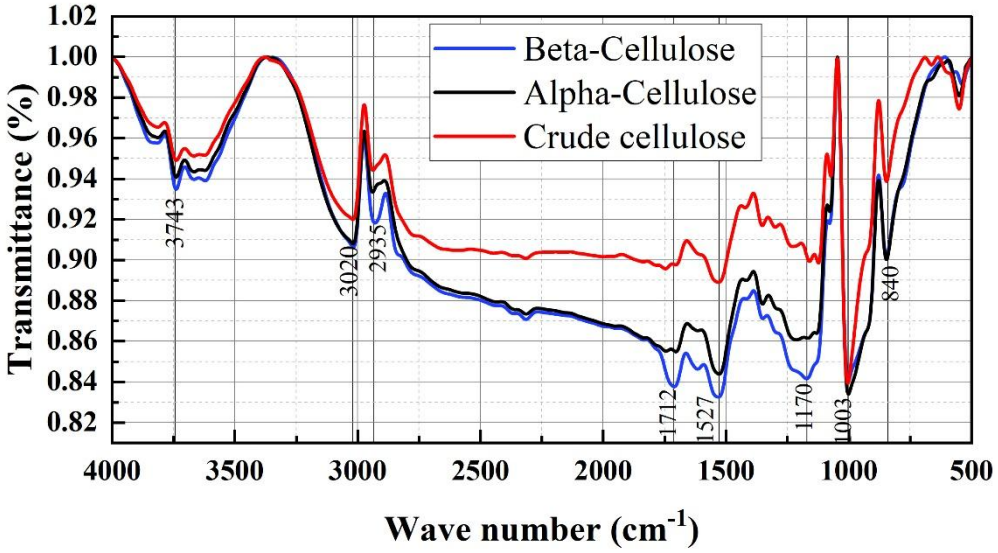

Fig. 3 FTIR graph of Cellulose

3.4 X-ray diffraction (XRD) analysis

Fig. 4 shows the X-ray diffraction (XRD) profiles of the Crude cellulose, α, and β-cellulose samples. The structural makeup of cellulose comprises both crystalline and amorphous portions. The crystalline planes of lattice 110, 200, and 004 can be identified by the three different peak shapes that the three cellulose samples produced at 16.42°, 31.34°, and 42.82°, respectively [38]. Although there currently is no doublet in the intensity of the main peak, the XRD diffraction data of all the samples confirmed their contents comprised native cellulose I and were not composed of cellulose II. Cellulose's crystallinity index and the size of its crystals have an enormous effect on its stability at its temperatures.[39] The total amount of crystalline and amorphous cellulosic components in a sample can be detected by using XRD to determine cellulose's crystallinity index (C.I.). In addition, the size of the crystallites contributes to understanding the cellulose's crystallinity. Table 1 provides data on each sample's crystallinity index, crystallite size, and thermal decomposition. The crystallinity index for the β-cellulose was found to be high (C.I. = 79.10%). Crude cellulose and α-cellulose have been found with a crystallinity index of 71.35% and 63.05%, accordingly. It was quite noteworthy to notice that all three samples' crystallite sizes were in a comparable order as C.I., indicating that β-cellulose's crystallite size (51.67 nm) was larger than that of Crude cellulose (38.27 nm) and α-cellulose (18.54 nm). thereby, we could contend that crystallite size might be correlated with an increase in the crystalline region, or conversely.[40]

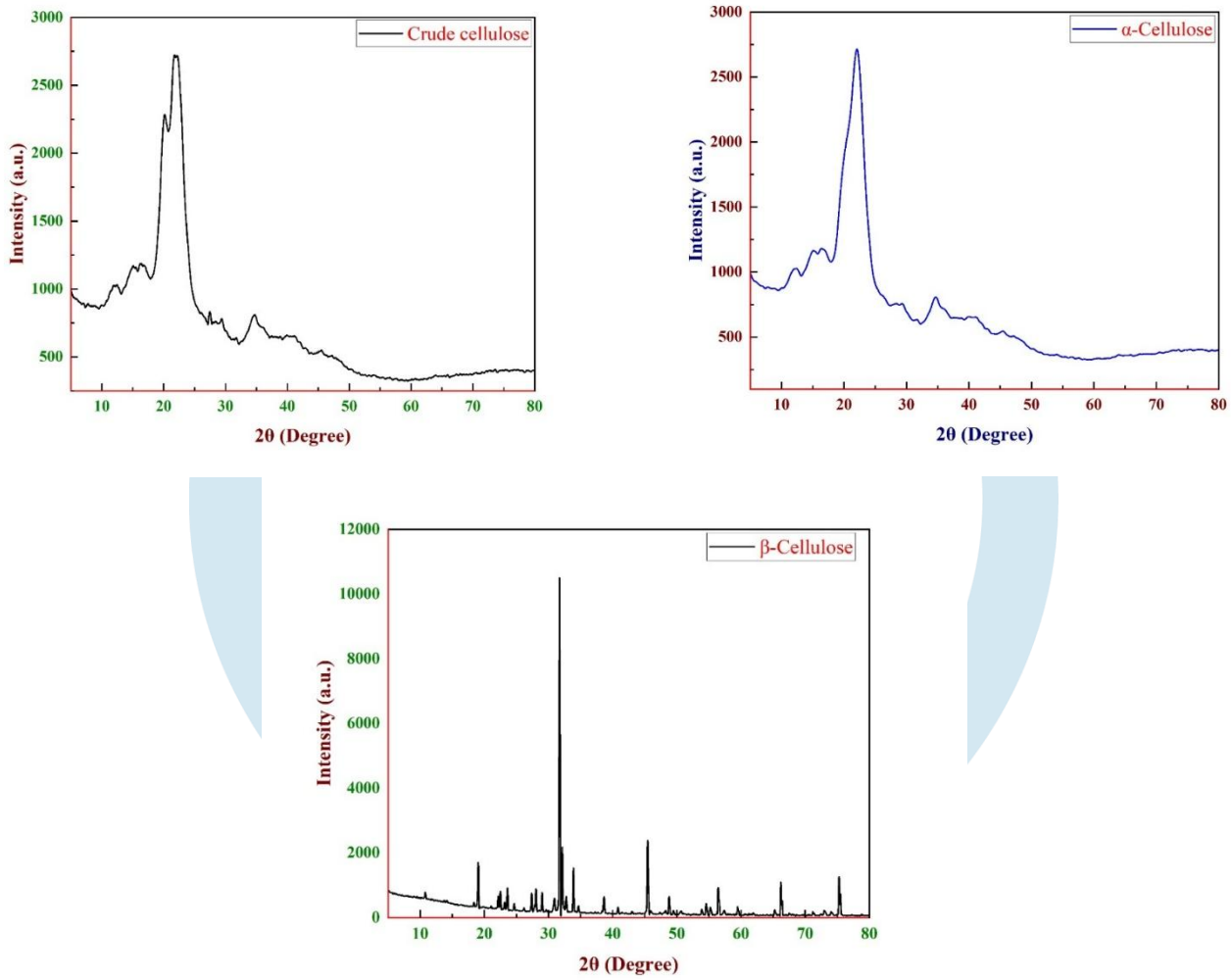

Fig. 4 XRD graph of Cellulose

3.5 Thermogravimetric (TGA) analysis

Thermogravimetric analysis was implemented to figure out each sample's thermal durability. The impact of heating and subsequently pyrolytic the decomposition of crude cellulose, α-, and β-cellulose can be seen in **Fig. 5**. For α- and β-cellulose, the beginning of breakdown started around 25 and 240°C, which led to an initial weight loss that was approximately 11.38% and 3.93%, accordingly. This came because of the loss of water, which had been dispersed on the cellulose's surface.[41] At 200°C, the α and β-cellulose began to break down. In the 200-500°C temperature range, α-cellulose degrades, indicating a mass reduction of about 23.37%. β-cellulose breaks through two phases. In the first phase, which was carried out at ranges from 200° and 500°C, only approximately 64.3% of the mass was lost. In the second phase, a decrease in mass of approximately 6.33% was found in the 500°–750°C temperature region. The existence of different parts that are broken down at temperatures that vary can be seen by the various phases of the crude cellulose degradation. Approximately 7.26%, 2.66% (9.92%) of the mass was lost up to 200°C, most probably as an effect of humidity evaporation. Crude cellulose began to break down at 200°C and did so in three phases. In

the first phase, between 250° and 400°C, there was a reduction in mass of approximately 58.94%. A temperature range between 400° to 600° indicates a decrease in mass of approximately 7.89% in the second phase. A temperature ranging from 600° to 800° showed a decrease in mass of approximately 4.13% in the third phase.

Fig. 5 TGA graph of cellulose

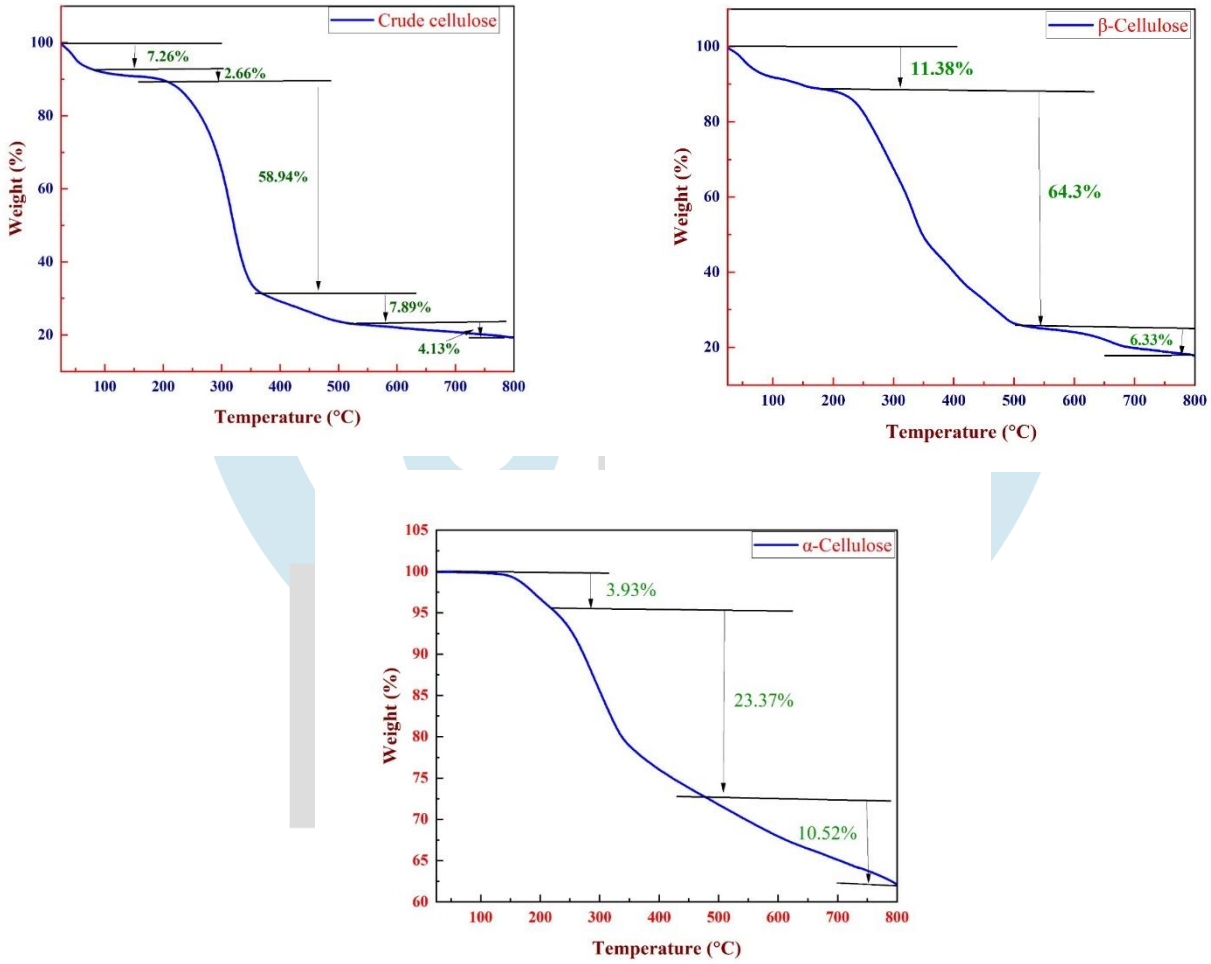

Under a thermal investigation of α- and β-cellulose, β-cellulose is more resistant to degradation than α-cellulose, whilst α-cellulose exhibits a considerable decrease in mass 23.37% (~24%) and β-cellulose exhibits no discernible degradation (~2%). Additionally, β-cellulose tends to be more resistant to thermal degradation than α-cellulose according to the results of the crystallinity index and crystallite size from the XRD results

4. CONCLUSION

In this study, cellulose was extracted from *Sericostoma Pauciflorum*, commonly referred to as "Karvas" through a process involving bleaching, followed by treatments with alkali and acid. The crude cellulose obtained was then separated into α and β-cellulose fractions. The crude cellulose content in *Sericostoma Pauciflorum* was found to be 82%, with α and β-cellulose contents being 83.6% and 8.2%, respectively, indicating a predominance of α-cellulose. Analyses using SEM and FTIR confirmed the removal of most Crude cellulose and lignin during the extraction process and provided evidence of successful cellulose isolation. XRD analysis revealed the presence of only the cellulose I polymorph structure, with no cellulose

II detected. The crystallinity index and crystallite size of β-cellulose (79.10% and 51.67 nm, respectively) were higher than those of α-cellulose (63.05% and 18.54 nm). An increase in crystallinity was also observed in β-cellulose (79.10%) compared to crude cellulose (71.35%). TGA demonstrated that β-cellulose exhibited significantly greater thermal stability than α-cellulose. The thermal decomposition of α and β-cellulose within the temperature range of 200-°C was recorded at 64.3% and 6.33%, respectively. These findings were consistent with existing literature. Although many researchers have isolated cellulose using various methods and sources, there appears to be a lack of studies on the fractionation of native cellulose and its chemical characterization. Therefore, the primary aim of this research was to fractionate native cellulose using a cost-effective method and to analyse the chemical characteristics of the fractionated cellulose to explore their potential applications in various fields.

5. ACKNOWLEDGEMENTS

The authors express their appreciation to Dr. Ajay Sharma, Principal of Government. College, Sirohi

6. AUTHOR CONTRIBUTIONS

Conceptualization and Supervision – Dr. Hardik Bhatt,

Investigation, writing, and editing Jitubhai Morabiya and Sanjay Bamaniya.

All authors have read and agreed to the published version of the manuscript.

7. CONFLICT OF INTEREST

The authors declare no conflict of interest.

8. ETHICS APPROVAL

This work was completely self-investigated, and all generated data by self-diagnosis are from the Google Scholar literature survey. Given that all the figures are drawn by the author, further no need for any approval.

9. FUNDING

It is certified that researchers did not receive any grant from funding agencies in the public, commercial, or non-revenue-driven sectors.

10. REFERENCES

[1] Lopez, G., Keiner, D., Fasihi, M., Koiranen, T., & Breyer, C. (2023). From fossil to green chemicals: Sustainable pathways and new carbon feedstocks for the global chemical industry. Energy & Environmental Science, 16(7), 2879–2909. https://doi.org/ 10.1039/D3EE00478C

[2] Alila, S., Besbes, I., Vilar, M. R., Mutj´ e, P., & Boufi, S. (2013). Non-woody plants as raw materials for production of microfibrillated cellulose (MFC): A comparative study. Industrial Crops and Products, 41(1), 250–259. https://doi.org/10.1016/J. INDCROP.2012.04.028

[3] Sankhla, S., Sardar, H. H., & Neogi, S. (2021). Greener extraction of highly crystalline and thermally stable cellulose micro-fibers from sugarcane bagasse for cellulose nano-fibrils preparation. Carbohydrate Polymers, 251, 117030. https://doi.org/ 10.1016/J.CARBPOL.2020.117030

[4] Zheng, M., Chen, J., Tan, K. B., Chen, M., & Zhu, Y. (2022). Development of hydroxypropyl methylcellulose film with xanthan gum and its application as an excellent food packaging bio-material in enhancing the shelf life of banana. Food Chemistry, 374, 131794. https://doi.org/10.1016/J.FOODCHEM.2021.131794

[5] Li, X., C. Wan, T. Tao, H. Chai, Q. Huang, Y. Chai, Y. Wu, et al. 2024. "An Overview of the Development Status and Applications of Cellulose-Based Functional Materials." Cellulose 31 (1): 61–99. https://doi.org/10.1007/s10570-023- 05616-8

[6] Eichhorn, S. J., Dufresne, A., Aranguren, M., Marcovich, N. E., Capadona, J. R., Rowan, S. J., Weder, C., Thielemans, W., Roman, M., Renneckar, S., Gindl, W., Veigel, S., Keckes, J., Yano, H., Abe, K., Nogi, M., Nakagaito, A. N., Mangalam, A., Simonsen, J., . . . Peijs, T. (2009). Review: current international research into cellulose nanofibres and nanocomposites. Journal of Materials Science, 45(1), 1–33. https://doi.org/10.1007/s10853-009-3874-0

[7] Klemm, D., Heublein, B., Fink, H., & Bohn, A. (2005). Cellulose: fascinating biopolymer and sustainable raw material. Angewandte Chemie International Edition, 44(22), 3358–3393. https://doi.org/10.1002/anie.200460587

[8] Plaza, P. E., Gallego-Morales, L. J., Pe˜nuela-V´asquez, M., Lucas, S., García-Cubero, M. T., & Coca, M. (2017). Biobutanol production from brewer's spent grain hydrolysates by Clostridium beijerinckii. Bioresource Technology, 244, 166–174. https://doi.org/10.1016/J.BIORTECH.2017.07.139

[9] Vergara, P., Ladero, M., Garcia-Ochoa, F., & Technology, J. V.-B. Pre-treatment of corn stover, Cynara cardunculus L. stems and wheat straw by ethanol-water and diluted sulfuric acid: Comparison under different energy. Elsevier. https://www.sciencedirect.com/science/article/pii/S0960852418313117

[10] Saratale, R. G., Saratale, G. D., Cho, S. K., Kim, D. S., Ghodake, G. S., Kadam, A., & Shin, H. S. (2019). Pretreatment of kenaf (Hibiscus cannabinus L.) biomass feedstock for polyhydroxybutyrate (PHB) production and characterization. Bioresource Technology, 282, 75–80. https://doi.org/10.1016/j.biortech.2019.02.083

[11] Lai, C., Yang, C., Zhao, Y., Jia, Y., Chen, L., Zhou, C., & Yong, Q. (2020). Promoting enzymatic saccharification of organosolv-pretreated poplar sawdust by saponin-rich tea seed waste. Bioprocess and Biosystems Engineering, 43(11), 1999–2007. https://doi.org/10.1007/S00449-020-02388-4

[12] Singh, J., Sharma, A., Sharma, P., Singh, S., Das, D., Chawla, G., & Nain, L. (2020). Valorization of jute (Corchorus sp.) biomass for bioethanol production. Biomass Conversion and Biorefinery. https://doi.org/10.1007/S13399-020-00937-1.

[13] Ajala, E. O., Ighalo, J. O., Ajala, M. A., Adeniyi, A. G., & Ayanshola, A. M. (2021). Sugarcane bagasse: a biomass sufficiently applied for improving global energy, environment and economic sustainability. Bioresources and Bioprocessing, 8(1), 1–25. https://doi.org/10.1186/S40643-021-00440-Z.

[14] Pennells, J., Cruickshank, A., Chal´eat, C., Godwin, I. D., & Martin, D. J. (2021). Sorghum as a novel biomass for the sustainable production of cellulose nanofibers. Industrial Crops and Products (p. 171). https://doi.org/10.1016/j.indcrop.2021.113917.

[15] Sun, B., Zhang, M., Hou, Q., Liu, R., Wu, T., & Si, C. (2016). Further characterization of cellulose nanocrystal (CNC) preparation from sulfuric acid hydrolysis of cotton f ibers. Cellulose, 23(1), 439–450. https://doi.org/10.1007/s10570-015-0803-z

[16] Vizireanu, S., Panaitescu, D. M., Nicolae, C. A., Frone, A. N., Chiulan, I., Ionita, M. D., Satulu, V., Carpen, L. G., Petrescu, S., Birjega, R., & Dinescu, G. (2018). Cellulose defibrillation and functionalization by plasma in liquid treatment. *Scientific Reports*, *8*(1). https://doi.org/10.1038/s41598-018-33687-2

[17] Peng, Z., Lin, Q., Tai, Y.-A. A., & Wang, Y. (2020). Applications of Cellulose Nanomaterials in Stimuli-Responsive Optics [Review of Applications of Cellulose Nanomaterials in Stimuli-Responsive Optics]. Journal of Agricultural and Food Chemistry, 68(46), 12940. American Chemical Society. https://doi.org/10.1021/acs.jafc.0c04742

[18] Fredricks, J. L., Jimenez, A. M., Grandgeorge, P., Meidl, R., Law, E., Fan, J., & Roumeli, E. (2023). Hierarchical biopolymer-based materials and composites. *Journal of Polymer Science*, *61*(21), 2585–2632. https://doi.org/10.1002/pol.20230126

[19] Pandey, A., M. K. Singh, and A. Singh. 2024. "Bacterial Cellulose: A Smart Biomaterial for Biomedical Applications." Journal of Materials Research 39 (1): 2–18. https://doi.org/10.1557/s43578-023-01116-4

[20] Baghel, R. S., Reddy, C., & Singh, R. P. (2021). Seaweed-based cellulose: Applications, and future perspectives. *Carbohydrate Polymers*, *267*, 118241. https://doi.org/10.1016/j.carbpol.2021.118241

[21] Rahman, M. R., Hasan, M., Huque, M. M., & Islam, M. N. (2009). Physico-Mechanical properties of Jute Fiber reinforced polypropylene composites. *Journal of Reinforced Plastics and Composites*, *29*(3), 445–455. https://doi.org/10.1177/0731684408098008

[22] Doh, H., Lee, M. H., & Whiteside, W. S. (2019). Physicochemical characteristics of cellulose nanocrystals isolated from seaweed biomass. *Food Hydrocolloids*, *102*, 105542. https://doi.org/10.1016/j.foodhyd.2019.105542

[23] Siddhanta, A. K., Chhatbar, M. U., Mehta, G. K., Sanandiya, N. D., Kumar, S., Oza, M. D., Prasad, K., & Meena, R. (2010). The cellulose contents of Indian seaweeds. In Journal of Applied Phycology (Vol. 23, Issue 5, p. 919). Springer Science+ Business Media. https://doi.org/10.1007/s10811-010-9599-2

[24] Or, T., Miettunen, K., Cranston, E. D., Moran-Mirabal, J. M., & Vapaavuori, J. (2019). Cellulose nanocrystal aerogels as electrolyte scaffolds for glass and plastic Dye-Sensitized solar cells. *ACS Applied Energy Materials*, *2*(8), 5635–5642. https://doi.org/10.1021/acsaem.9b00795

[25] Surolia, P. K., & Jasra, R. V. (2016). Photocatalytic degradation of p-nitrotoluene(PNT) using TiO_2-modified sil-exchanged NaY zeolite: Kinetic study and identification of mineralization pathway. *Desalination and Water Treatment, 57(46), 22081-22098.* https://doi.org/10.1080/19443994.2015.1125798

[26] Trache, D., Thakur, V. K., & Boukherroub, R. (2020). Cellulose Nanocrystals/Graphene Hybrids—A promising new class of materials for advanced applications. *Nanomaterials*, *10*(8), 1523. https://doi.org/10.3390/nano10081523

[27] Ahmed, E. M. (2015). Hydrogel: Preparation, characterization, and applications: A review. Journal of Advanced Research, 6(2), 105–121. https://doi.org/10.1016/J.JARE.2013.07.006

[28] Chai, Q., Jiao, Y., & Yu, X. (2017). Hydrogels for Biomedical Applications: Their Characteristics and the Mechanisms behind Them. Gels, 3(1). https://doi.org/10.3390/GELS3010006

[29] Mihranyan, A., Llagostera, A. P., Karmhag, R., Strømme, M., & Ek, R. (2003). Moisture sorption by cellulose powders of varying crystallinity. *International Journal of Pharmaceutics*, *269*(2), 433–442. https://doi.org/10.1016/j.ijpharm.2003.09.030

[30] Siddhanta, A., Prasad, K., Meena, R., Prasad, G., Mehta, G. K., Chhatbar, M. U., Oza, M. D., Kumar, S., & Sanandiya, N. D. (2009). Profiling of cellulose content in Indian seaweed species. *Bioresource Technology*, *100*(24), 6669–6673. https://doi.org/10.1016/j.biortech.2009.07.047

[31] Parihar, D., Kumar, M., Gehlot, P. S., Surolia, P. K., & Prasad, G. (2021). Extraction and Characterization of Fractionated Cellulose from Acacia Senegal. *Journal of Natural Fibers*, *19*(15), 10499–10512. https://doi.org/10.1080/15440478.2021.1994092

[32] Patterson, A. L. (1939). The Scherrer formula for X-Ray particle size determination. *Physical Review*, *56*(10), 978–982. https://doi.org/10.1103/physrev.56.978

[33] Poletto, M., Pistor, V., Zeni, M., & Zattera, A. J. (2010). Crystalline properties and decomposition kinetics of cellulose fibers in wood pulp obtained by two pulping processes. *Polymer Degradation and Stability*, *96*(4), 679–685. https://doi.org/10.1016/j.polymdegradstab.2010.12.007

[34] Alemdar, A., & Sain, M. (2007). Isolation and characterization of nanofibers from agricultural residues – Wheat straw and soy hulls. *Bioresource Technology*, *99*(6), 1664–1671. https://doi.org/10.1016/j.biortech.2007.04.029

[35] Troedec, M. L., Sedan, D., Peyratout, C., Bonnet, J. P., Smith, A., Guinebretiere, R., Gloaguen, V., & Krausz, P. (2007). Influence of various chemical treatments on the composition and structure of hemp fibres. *Composites Part a Applied Science and Manufacturing*, *39*(3), 514–522. https://doi.org/10.1016/j.compositesa.2007.12.001

[36] De Oliveira, J. P., Bruni, G. P., Lima, K. O., Halal, S. L. M. E., Da Rosa, G. S., Dias, A. R. G., & Da Rosa Zavareze, E. (2016). Cellulose fibers extracted from rice and oat husks and their application in hydrogel. *Food Chemistry*, *221*, 153–160. https://doi.org/10.1016/j.foodchem.2016.10.048

[37] Sun, X., Xu, F., Sun, R., Fowler, P., & Baird. (2004). Characteristics of degraded cellulose obtained from steam-exploded wheat straw. *Carbohydrate Research*, *340*(1), 97–106. https://doi.org/10.1016/j.carres.2004.10.022

[38] Jordan, J. H., M. W. Easson, B. Dien, S. Thompson, and B. D. Condon. 2019. "Extraction and Characterization of Nanocellulose Crystals from Cotton Gin Motes and Cotton Gin Waste." Cellulose 26 (10): 5959–5979. https://doi.org/ 10.1007/s10570-019-02533-7

[39] Rojas, O. J. (2016). Cellulose chemistry and properties: fibers, nanocelluloses and advanced materials. In *Advances in polymer science*. https://doi.org/10.1007/978-3-319-26015-0

[40] Prasanna, N. S., & Mitra, J. (2020). Isolation and characterization of cellulose nanocrystals from Cucumis sativus peels. *Carbohydrate Polymers*, *247*, 116706. https://doi.org/10.1016/j.carbpol.2020.116706

[41] Pacaphol, K., Seraypheap, K., & Aht-Ong, D. (2023). Extraction and Silylation of Cellulose Nanofibers from Agricultural Bamboo Leaf Waste for Hydrophobic Coating on Paper. *Journal of Natural Fibers*, *20*(1). https://doi.org/10.1080/15440478.2023.2178581